Catal Lett (2009) 130:222–226
DOI 10.1007/s10562-009-9868-3

Photooxidation of Oxalic Acid on Sm_2O_3: Synergism by Semiconductors

C. Karunakaran · R. Dhanalakshmi · P. Anilkumar

Received: 9 September 2008 / Accepted: 13 January 2009 / Published online: 4 February 2009

Abstract Oxalic acid is photooxidized on Sm_2O_3 and the oxidation follows first-order kinetics with a linear dependence on light intensity. The photocatalytic efficiency is higher with UV-C light than with UV-A light. While TiO_2, ZnO, CuO, Bi_2O_3 and Nb_2O_5 individually photocatalyze the oxidation each semiconductor exhibits synergistic effect when present along with Sm_2O_3 indicating interparticle electron-jump from oxalic acid adsorbed Sm_2O_3 to the band gap-excited semiconductor on collision. The ease of photooxidation of the acids on Sm_2O_3 is: formic > oxalic > acetic > citric.

Keywords Insulator · Semiconductor · Interparticle electron-jump · Photocatalysis

1 Introduction

Band gap excitation of semiconductors generates electron–hole pairs, holes in the valence band and electrons in the conduction band. A fraction of these electron–hole pairs takes part in chemical reactions with electron donors and acceptors, leading to photocatalysis. But we report here for the first time photoreaction on the surface of Sm_2O_3, a ceramic; the extensively investigated mineralization of oxalic acid is the test reaction taken up for the study [1–9]. Also, our results reveal that the oxalic acid oxidation on Sm_2O_3 is enhanced by semiconductors, an unusual synergism when a semiconductor is present along with an insulator. Reports on interparticle charge-transfer between semiconductors are many; while a couple of studies are on charge-transfer between two particulate semiconductors [10, 11] others are in coupled semiconductors [12, 13].

C. Karunakaran (✉) · R. Dhanalakshmi · P. Anilkumar
Department of Chemistry, Annamalai University, Annamalainagar, Tamilnadu 608002, India
e-mail: karunakaranc@rediffmail.com

2 Experimental

Sm_2O_3 (Sd fine), TiO_2 (Merck), ZnO (Merck), CuO (Sd fine), Bi_2O_3 (Sd fine), Nb_2O_5 (Sd fine) and Al_2O_3 (Merck) were of analytical grade and used as supplied.

Photooxidation was carried out in a multilamp photoreactor fitted with eight 8 W mercury lamps of wavelength 365 nm (Sankyo Denki, Japan), a highly polished anodized aluminum reflector and four cooling fans. Borosilicate glass tube of 15 mm inner diameter was used as the reaction vessel and was placed at the centre. The light intensity was varied by using two, four and eight lamps with the angle sustained by the adjacent lamps at the sample as 180, 90 and 45°, respectively. The reaction was also studied in a micro-photoreactor fitted with a 6 W 254 nm low-pressure mercury lamp and a 6 W 365 nm mercury lamp. Quartz and borosilicate glass tubes were used for 254 and 365 nm lamps, respectively. The photon flux (I) of the light source was determined under identical experimental conditions by ferrioxalate actinometry.

The photooxidation was carried out with 25 and 10 mL of oxalic acid solutions in the multilamp and micro-photoreactors, respectively. The solutions were purged with air that effectively kept the added catalyst under suspension and at continuous motion; the airflow rate was measured by soap bubble method. After illumination, the oxide was recovered by centrifugation and the unoxidized oxalic acid was analyzed by alkalimetry and also by permanganometry [1, 6], both results were identical. The decrease in acid concentration for a finite time of illumination provided the

reaction rate which was reproducible to ±5%. A time lag of at least 15 min was provided prior to illumination to ensure pre-adsorption of the acid on the oxide. The dissolved O_2 was measured using Elico dissolved oxygen analyzer PE 135, Avatar 330FT-IR spectrometer was used to record the infrared spectra and the diffuse reflectance spectra were obtained using Shimadzu UV-2450 UV-Visible spectrometer with $BaSO_4$ as reference. Pre-sonication was made with Toshcon SW 2 ultrasonic bath (37 ± 3 kHz, 150 W).

3 Results and Discussion

The TiO_2 used is of anatase phase; the XRD pattern of the sample is identical with the standard pattern of anatase (JCPDS 00-021-1272*) and the rutile lines (00-034-0180 D) are absent (Siemens D-5000 XRD, CuK_α X-ray, $\lambda = 1.54$ Å, scan: 5–60°, scan speed: 0.2° s^{-1}). The XRD of ZnO is that of the JCPDS pattern (00-005-0664 D) of zincite (Bruker D8 XRD, CuK_α X-ray, $\lambda = 1.5406$ Å scan: 5–70°, scan speed: 0.050° s^{-1}). The diffraction pattern of Al_2O_3 matches with the standard JCPDS patterns of γ-Al_2O_3 (00-001-1308 D, cubic: *a* 7.900, *b* 7.900, *c* 7.900 Å, α 90.0°, *β* 90.0°, *γ* 90.0°) and χ-Al_2O_3 (00-004-0880 N, cubic: *a* 7.950, *b* 7.950, *c* 7.950 Å, α 90.0°, *β* 90.0°, *γ* 90.0°) revealing the presence of both the phases (γ:χ::52:48). The particle sizes, determined using particle sizer Horiba LA-910 or Malvern 3600E (focal length 100 mm, beam length 2.0 mm, wet (methanol) presentation), are: TiO_2: 2.6–27.6, ZnO: 3.5–27.6, CuO: 5.69–30.5, Bi_2O_3: 0.17–0.49, Nb_2O_5: 0.22–0.43, Al_2O_3: 2.6–57.7 μm. The BET surface areas were determined as: TiO_2: 14.68, ZnO: 12.16, CuO: 1.51, Bi_2O_3: 2.75, Nb_2O_5: 1.94, Al_2O_3: 10.63 m^2 g^{-1}.

In presence of air under UV light, oxalic acid is oxidized on the surface of Sm_2O_3 and the influence of reaction parameters like illumination time, oxalic acid concentration, catalyst loading and photon flux on the photoreaction was investigated using the multilamp photoreactor with mercury lamps of wavelength 365 nm. Oxalic acid gets adsorbed over Sm_2O_3 and the infrared spectrum of Sm_2O_3 which was recovered from oxalic acid solution prior to illumination and dried at 100 °C shows characteristic absorbance around 1,640 and 3,440 cm^{-1}. The adsorption of oxalic acid at 0.01 M under the conditions reported in Fig. 1 is 5% while the photooxidation in 30 min is 57%; the photooxidation results were corrected for adsorption. Sm_2O_3 does not lose its activity on repeated usage. The recycled catalyst without any pre-treatment shows identical photocatalytic activity. The exponential decrease of oxalic acid concentration with illumination time reveals first-order kinetics and in absence of Sm_2O_3 the oxidation is

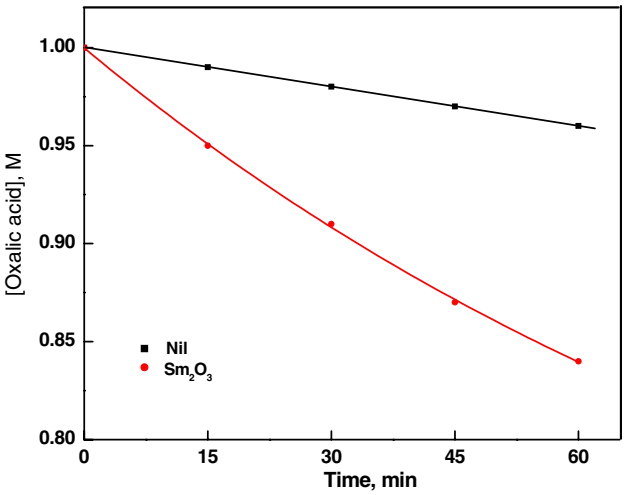

Fig. 1 Photooxidation of oxalic acid on Sm_2O_3: concentration–time profile. Sm_2O_3 loading = 0.050 g, airflow rate = 7.8 mL s^{-1}, $[O_2]_{dissolved}$ = 24.7 mg L^{-1}, oxalic acid solution = 25 mL, λ = 365 nm, I = 25.4 μEinstein L^{-1} s^{-1}

small (Fig. 1). There is no loss of oxalic acid due to air-purging. Determination of the photooxidation rates at different oxalic acid concentrations reveals linear increase of the reaction rate with oxalic acid concentration confirming the first-order kinetics (Fig. 2). Also, the photooxidation rate increases linearly with photon flux (Fig. 3); the loss of oxalic acid due to photolysis is small. Calculation of the photonic efficiency (ξ) shows that it does not vary significantly with the light intensity (31.5 ± 0.4%; conditions as in Fig. 3). The efficiency of oxidation is moderately enhanced by increasing the catalyst loading; doubling the catalyst loading from 0.050 to 0.10 g improves the

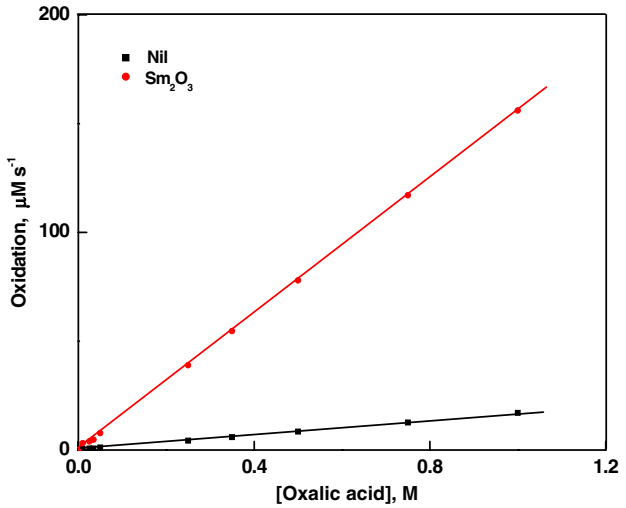

Fig. 2 Photooxidation as a function of concentration. Sm_2O_3 loading = 0.050 g, airflow rate = 7.8 mL s^{-1}, $[O_2]_{dissolved}$ = 24.7 mg L^{-1}, oxalic acid solution = 25 mL, λ = 365 nm, I = 25.4 μEinstein L^{-1} s^{-1}

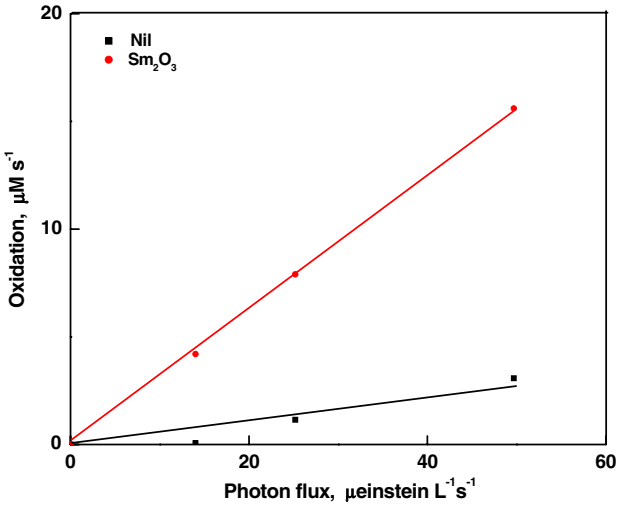

Fig. 3 Photooxidation as a function of photon flux. $[\text{oxalic acid}]_0 = 0.050$ M, Sm_2O_3 loading = 0.050 g, $[O_2]_{\text{dissolved}} = 24.7$ mg L^{-1}, airflow rate = 7.8 mL s^{-1}, oxalic acid solution = 25 mL, $\lambda = 365$ nm

photonic efficiency to 54% (conditions as in Fig. 3 but at light intensity of 25.4 μEinstein L^{-1} s^{-1}). Study of the oxidation using a 6 W 365 nm mercury lamp and a 6 W 254 nm low-pressure mercury lamp separately in the micro-reactor under identical conditions shows that UV-C light is more efficient than UV-A light to oxidize oxalic acid; the photonic efficiencies of oxidation with illumination at 365 and 254 nm are 66.4 and 75.4%, respectively (10 mL 0.050 M oxalic acid, 0.050 g Sm_2O_3 loading, 7.8 mL s^{-1} airflow rate, 24.7 mg L^{-1} dissolved O_2). Dissolved O_2 is essential for the photooxidation; deaeration of oxalic acid solution by N_2-purging instead of air arrests the oxidation (conditions as in Fig. 3 with photon flux of 25.4 μEinstein L^{-1} s^{-1} and 24.7 and 3.3 mg L^{-1} dissolved O_2 in air- and N_2-purged solutions, respectively). Anions like Cl^-, Br^-, SO_4^{2-} and NO_3^- do not interfere in the photoprocess. Vinyl monomers like acryl amide and acrylonitrile (5 mM) neither suppress the photonic efficiency nor get polymerized indicating the absence of chain carrier in the solution phase. Anionic as well as cationic micelles like aerosol OT, sodium lauryl sulfate and cetyltrimethylammonium bromide (5 mM) do not suppress the photonic efficiency which suggests that the photooxidation rate is not determined by reactions in solution. Azide ion, a $^1O_2$ quencher, fails to inhibit the oxidation indicating the absence of involvement of $^1O_2$ in the photoprocess. Generally, the photocatalytic activity is susceptible to the surface and size modification of the catalyst particles. Sonication in aqueous solution causes rapid formation, growth and collapse of cavities resulting in local high pressures and temperatures that are responsible for surface and particle size modification of the catalyst [14]. However, pre-sonication does not alter the photocatalytic activity; Sm_2O_3-catalyzed oxalic acid oxidation rate is not significantly altered by pre-sonication for 10 min at 37 ± 3 kHz and 150 W. While oxalic acid is easily photooxidized oxalate ion resists the same; the photonic efficiency of oxidation of oxalate ion under the conditions stated in Fig. 3 with photon flux of 25.4 μEinstein L^{-1} s^{-1} is 4.4% compared to 31.5% of oxalic acid. This suggests that it is the undissociated acid but not the anion that gets adsorbed over Sm_2O_3 and undergoes oxidation.

Oxalic acid is adsorbed on Sm_2O_3. The acidic sites on the surface of Sm_2O_3 may coordinate to the carbonyl oxygen and/or the basic O^- group may be involved in hydrogen bonding with the –OH group of the carboxylic acid. The possible mechanism is the absorption of light by oxalic acid adsorbed on Sm_2O_3 leading to its excitation. The diffuse reflectance spectra of oxalic acid-adsorbed Sm_2O_3 and bare Sm_2O_3 confirm the same. While oxalic acid-adsorbed Sm_2O_3 absorbs light at the wavelength of illumination the bare Sm_2O_3 fails to do so (Fig. 4). Transfer of the excited electron to a neighboring adsorbed oxygen molecule may initiate the degradation of oxalic acid. The proposed mechanism is supported by the report that 2,4,5-trichlorophenol forms a charge–transfer complex with TiO_2 which is activated by light of wavelength as long as 520 nm resulting in photochemical reaction [15]. The fact that the reaction fails to occur in absence of oxygen is in agreement with the suggested mechanism.

The Langmuir–Hinshelwood kinetic law is applicable to photooxidation and hence [16]:

$$rate = kK_1K_2ICS[\text{acid}][O_2]/(1 + K_1[\text{acid}])(1 + K_2[O_2])$$

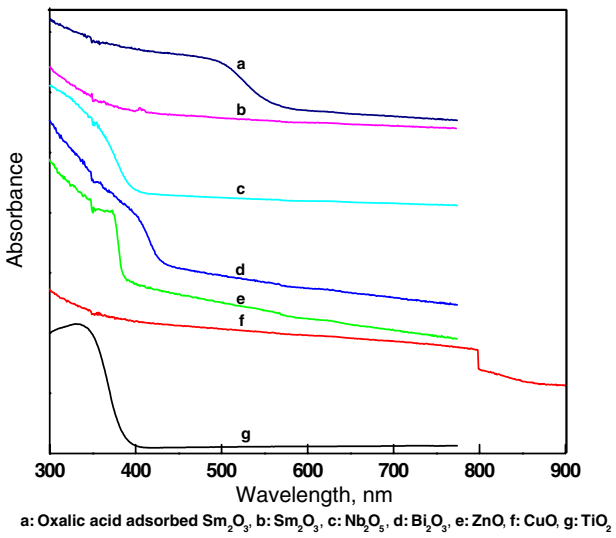

Fig. 4 Diffuse reflectance spectra

where K_1 and K_2 are the adsorption coefficients of oxalic acid and molecular oxygen on the illuminated surface of Sm_2O_3, k is the specific rate of oxidation, S is the specific surface area of Sm_3O_3, C is Sm_2O_3-loading per litre and I is the light intensity in Einstein L^{-1} s^{-1}. As the acid solution was oxygen-saturated by continuous air-purging the dissolved oxygen concentration remained constant during the photooxidation. Since K_2 is constant $K_2[O_2]/(1 + K_2[O_2])$ turns to be a constant. The Langmuir–Hinshelwood kinetic law is valid for the observed results provided the adsorption coefficient of the acid on the illuminated surface of Sm_2O_3 (K_1) is small so that $K_1[\text{acid}] \ll 1$. This reduces the Langmuir–Hinshelwood equation to a linear dependence of the oxidation rate on the acid concentration.

With UV light TiO_2, Nb_2O_5, CuO, ZnO and Bi_2O_3 catalyze the oxidation of oxalic acid. All the five semiconductors exhibit band gap excitation under UV-A light as seen from their diffuse reflectance spectra (Fig. 4). The measured rates of oxidation on TiO_2, Nb_2O_5, CuO, ZnO and Bi_2O_3 are 11.9, 13.2, 9.5, 16.7 and 8.0 μM s^{-1}, respectively (25 mL 0.05 M oxalic acid, 0.10 g catalyst loading, 7.8 mL s^{-1} airflow rate, 24.7 mg L^{-1} dissolved O_2, phenol solution = 25 mL, 25.4 μEinstein L^{-1} s^{-1} photon flux at 365 nm, 10 min illumination). As expected, under identical experimental conditions Al_2O_3, an insulator, does not mediate the photooxidation of oxalic acid.

Band gap-illumination of semiconductors in a mixture enables vectorial transfer of excited electrons and holes from one semiconductor to another leading to enhanced photocatalytic efficiency and improved photocatalysis by semiconductor mixtures is known [10, 11]. But what we report here is enhanced photocatalysis due to the presence of a particulate semiconductor with Sm_2O_3, both kept under suspension and at continuous motion by purging of air in the illuminated solution. All the five semiconductors used show the enhancement with Sm_2O_3 (Fig. 5). This is because of hole-transfer from the illuminated semiconductor to the oxalic acid molecule adsorbed on Sm_2O_3 during collision.

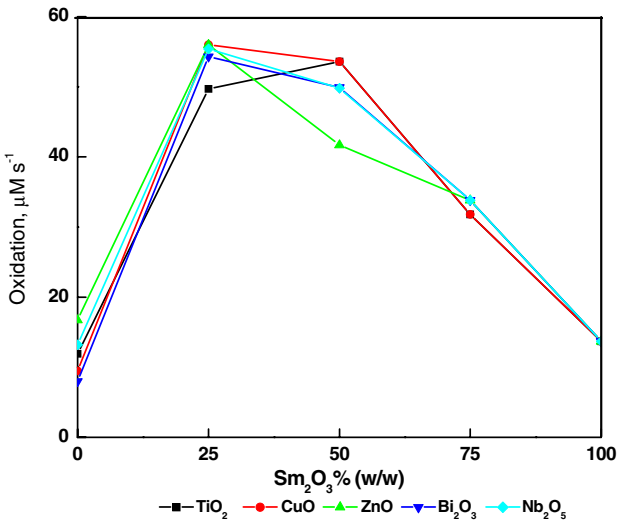

Fig. 5 Enhanced oxidation on Sm_2O_3 with semiconductors. [oxalic acid]$_0$ = 0.050 M, total catalyst loading = 0.10 g, airflow rate = 7.8 mL s^{-1}, $[O_2]_{dissolved}$ = 24.7 mg L^{-1}, oxalic acid solution = 25 mL, λ = 365 nm, I = 25.4 μEinstein L^{-1} s^{-1}

Sm_2O_3 effects the oxidation of formic, acetic and citric acids also under UV-A light and the ease of oxidation is: formic acid (91.4%) > oxalic acid (31.4%) > acetic acid (25.5%) > citric acid (3.0%); the values given in parenthesis are the photonic efficiencies under the conditions as in Fig. 5.

4 Conclusions

Sm_2O_3 mediates the oxidation of oxalic acid under UV-A light and the photonic efficiency is larger with UV-C light. The oxidation follows first-order kinetics on oxalic acid and shows linear dependence on photon flux. TiO_2, Nb_2O_5, CuO, ZnO and Bi_2O_3 individually photocatalyze the oxidation of oxalic acid and with Sm_2O_3 they show synergistic photocatalysis, an enhanced oxalic acid photooxidation, implying hole-transfer from the illuminated semiconductors to oxalic acid adsorbed on Sm_2O_3 during collision. The photonic efficiency of oxidation on Sm_2O_3 surface is of the order: formic acid > oxalic acid > acetic acid > citric acid.

Acknowledgments The authors thank the Council of Scientific and Industrial Research (CSIR), New Delhi, for the financial support through research Grant no. 01(2031)/06/EMR-II and R.D. is grateful to Annamalai University for UF.

References

1. Karunakaran C, Dhanalakshmi R (2008) Sol Energy Mater Sol Cells 92:588
2. Teoh WY, Amal R, Madler L, Pratsinis SE (2007) Cat Today 120:203
3. Iliev V, Tomova D, Bilyarska L, Tyuliev G (2007) J Mol Catal A 263:32
4. Iliev D, Tomova D, Bilyarska L, Eliyas A, Petrov L (2006) Appl Catal B 63:266
5. Sene JJ, Zeltner WA, Anderson MA (2003) J Phys Chem B 107:1597
6. Szabo-Bardos E, Czili H, Horvath A (2003) J Photochem Photobiol A 154:195
7. Franch MI, Ayllon JA, Peral J, Domenech X (2002) Catal. Today 76:221
8. Kosanic MM (1998) J Photochem Photobiol A 119:119
9. Kobayakawa K, Sato C, Sato Y, Fujishima A (1998) J Photochem Photobiol A 118:65
10. Serpone N, Maruthamuthu P, Pichat P, Pelizzetti E, Hidaka H (1995) J Photochem Photobiol A 85:247

11. Serpone N, Borgarello E, Gratzel M (1984) J Chem Soc Chem Commun 342
12. Kim KC, Han CS (2006) J Phys IV France 132:185
13. Bandara J, Tennakone K, Binduhewa P (2001) New J Chem 25:1302
14. Hirano K, Nitta H, Sawada K (2005) Ultrason Sonochem 12:271
15. Agrios AG, Gray KA, Weitz E (2003) Langmuir 19:1402
16. Karunakaran C, Senthilvelan S (2005) J Colloid Interface Sci 289:466